The 42nd International Technical Conference on Clean Energy

June 11-15, 2017, Clearwater, FL, USA

Technical Topic: Supercritical CO_2 Cycle

Materials and Manufacturing Challenges for Compact Heat Exchangers of Supercritical CO_2 Power Cycles

Ömer N. Doğan
Materials Research Engineer
National Energy Technology Laboratory
1450 Queen Avenue, S.W., Albany, OR, USA
omer.dogan@netl.doe.gov

Monica Kapoor
Postdoctoral Researcher
National Energy Technology Laboratory
1450 Queen Avenue, S.W., Albany, OR, USA
monica.kapoor@netl.doe.gov

Richard P. Oleksak
Postdoctoral Researcher
National Energy Technology Laboratory
1450 Queen Avenue, S.W., Albany, OR, USA
richard.oleksak@netl.doe.gov

Casey S. Carney
Research Scientist
National Energy Technology Lab and AECOM
1450 Queen Avenue, S.W., Albany, OR, USA
casey.carney@netl.doe.gov

Rajesh V. Saranam
Graduate Student
Mechanical, Industrial, and Manufacturing
Oregon State University, Corvallis, OR, USA
saranamv@oregonstate.edu

Patrick S. McNeff
Graduate Student
Mechanical, Industrial, and Manufacturing
Oregon State University, Corvallis, OR, USA
mcneffp@oregonstate.edu

Brian K. Paul
Professor
Mechanical, Industrial, and Manufacturing
Oregon State University,Corvallis, OR, USA
brian.paul@oregonstate.edu

Abstract: The supercritical CO_2 (sCO_2) power cycles rely heavily on heat recuperation to increase efficiency. Compact heat exchangers are proposed to reduce equipment size and enhance heat transfer between heat source and sCO_2**.** Microchannel architectures in these heat exchangers are typically formed by a lamination process wherein channels are formed in layers of sheet material, which are then stacked and joined together using diffusion bonding, brazing, or transient-liquid-phase bonding (TLPB). TLPB of Ni-based superalloy (Alloy 230) sheets into stacks was investigated. Electron microscopy identified solidification shrinkage porosity on the bond line as the most common defect in the TLP bonded stacks. Tensile yield strengths of 76-86 % of the base alloy strength were obtained on bonded stacks. Scanning electron microscopy on the fracture surfaces indicated ductile failure mode in the bonded zone. Environmental stability of joined regions in Alloy 230 stacks was investigated by exposing to CO_2 at 700°C for 1500 hours. Mass change and post-exposure microscopic analysis showed a corrosion behavior similar to the base material.

INTRODUCTION

Due to the potential for improved efficiencies in power generation, interest in sCO_2 cycles has increased in recent years. The sCO_2 cycles rely heavily on heat recuperation for increased efficiency. Compact heat exchanger (CHE) designs such as microchannel [Ghazvini], printed circuit [Le Pierres], microtubular, plate-fin, wire-mesh [Foursprings], and others are proposed to reduce equipment size and enhance heat transfer between the high-temperature and low-temperature working fluids in sCO_2 power cycles.

Components, containing small features, in CHEs are typically joined together by diffusion bonding, brazing, transient-liquid-phase bonding (TLPB), or laser welding. Diffusion bonding is a solid-state process that involves pressing layers of metallic materials at high temperatures (usually T > 0.5 * melting point) for several hours to form stacks. This results in closure of voids between the contacting surfaces through diffusional and creep processes eventually forming a continuous microstructure across the faying surfaces [Hill]. A thin layer of lower-melting-point alloy, containing a melting-point-depressing element (MPD), is placed between the joining surfaces before pressing at high temperatures in the case of brazing and TLPB. When this stack is heated, this thin layer melts and results in a transient-liquid-phase which facilitates bonding [Cook]. The difference between brazing and TLPB is that solidification of the interlayer takes place isothermally in TLPB as the MPD diffuses away from the interlayer whereas in the case of brazing, solidification is not isothermal. Although the goal is to form a monolithic structure, depending on the alloy composition and microstructure, the interface region of the bonded structure may have compositional and microstructural differences with respect to the parent alloy. This can be a source of mechanical and/or chemical instability for the structure in the application environments. Sometimes, post-bonding heat treatment may be practical to eliminate or reduce the chemical gradient and microstructural variation in the structure.

This paper examines the TLPB process of Alloy 230 for a CHE application. Microstructure, mechanical strength and environmental stability of the resulting TLP bonded structure are evaluated. Defects resulting from the TLPB process are identified.

EXPERIMENTAL PROCEDURE

For CHEs operating above 700˚C and 25 MPa in sCO2 environment, several Ni-based superalloys were reviewed. Among them, Alloy 230 was selected because of the following factors: (i) Although Alloy 230 is primarily a solid-solution-strengthened alloy, it contains high volume fraction of M_6C phase which is instrumental in pinning matrix grain boundaries at the high temperatures used in the bonding process. Alloy 230 is known as one of the most grain-growth-resistant material in the solid-solution-strengthened superalloy family, and (ii) Alloy 230 is also one of the most corrosion resistant alloys at high temperatures. Its composition is provided in Table 1.

Table 1. Nominal chemical composition of Alloy 230 in mass percent [Haynes 230 Technical Data]

Ni	Cr	W	Mo	Fe	Co	Mn	Si	Al	C	B
57	22	14	2	3	5	0.5	0.4	0.3	0.1	0.015

TLPB was investigated for fabrication of a CHE and involves the use of a low-melting-point plating (Ni-P alloy in this case), coated on the joining surfaces, which melts completely or partially at the bonding temperatures and facilitates the bonding [Cook]. Two sets of Alloy 230 stacks were bonded (Set I and

Set II). For both sets, the Alloy 230 sheets were bonded into stacks containing 100 sheets each with a thickness of ~ 550 µm and 14.5 cm^2 (2.25 in^2) cross-section. The sheets were coated with a 3µm Ni-P plating layer. The stacks were bonded at 1150°C for 4 h (Set II) to 8 h (Set I) at 12.7 MPa pressure in a vacuum chamber. The Ni-P plating alloy for Set I contained 12 mass percent P whereas that for Set II 6 mass percent. To mitigate the undesired effect of TLP bonding on the microstructure, a post-bonding heat treatment was applied to one stack of Set II. The treatment involved holding the bonded stacks for 1 hour at 1200°C followed by water quenching.

Vickers hardness testing was performed on a Beuhler Vicker's hardness tester under a 200 g load with a dwell time of 15 s. The reported hardness values are an average of ten values. Tensile tests were performed as specified in ASTM standard E8-13a [ASTM] in an Instron load frame. Solid cylindrical blank specimens were wire electrical-discharge-machined (EDM) from TLP bonded stacks. The tensile specimens gauge length of 22.86 mm (0.90 inch) and gauge diameter of 6.35 mm (0.25 inch) were machined from blanks such that the tensile loading was perpendicular to the bonding plane and along the short transverse direction of the Alloy 230 sheet. Tensile testing was performed at 750°C, which is close to the maximum operating temperature of these heat exchangers.

Corrosion coupons (15 mm x 10 mm x 1 mm) were machined from the stacks such that each coupon contained approximately 25 bonded layers. The coupons prepared from the as-received materials of Alloy 230 had the thickness of the sheet. After the coupons were placed in the furnace tube and the tube was sealed, the CO_2 flow was started 24 hours before the heating was begun. The coupons were exposed to ambient pressure CO_2, with a purity of 99.999%, at 700°C for 1500 hours. More details on the oxidation study can be found in [Doğan].

Optical microscopy and scanning electron microscopy (SEM) were utilized to study the general microstructure and composition of the Alloy 230 sheet and the joint region. SEM was performed at 20 KV on FEI Inspect F SEM. X-ray energy dispersive spectroscopy (EDS) composition analysis was performed to identify a composition gradient across the Alloy 230 sheet and joint region.

RESULTS AND DISCUSSION

Microstructure

To provide a perspective of the macrostructure of the TLP bonded stack –sheet and the joint –Fig. 1a shows a low magnification optical micrograph of cross section of etched Alloy 230 stack. The joint regions (labeled with arrows) which are also known as isothermally solidified zones (ISZ) are clearly delineated at a periodicity of approximately 530 µm, which is consistent with the thickness of Alloy 230 sheets. A few pores are observed along the joint region which are thought to form due to solidification-related shrinkage. Grain growth across the joint region, which is an indicator of a good quality joint is also observed. A closer look at the bond region (Fig. 1b) identifies distinct features of the bond and the base alloy. While the base alloy contains a significant volume fraction of M_6C (M = W, Mo, Ni) precipitates, the ISZ is denuded of them.

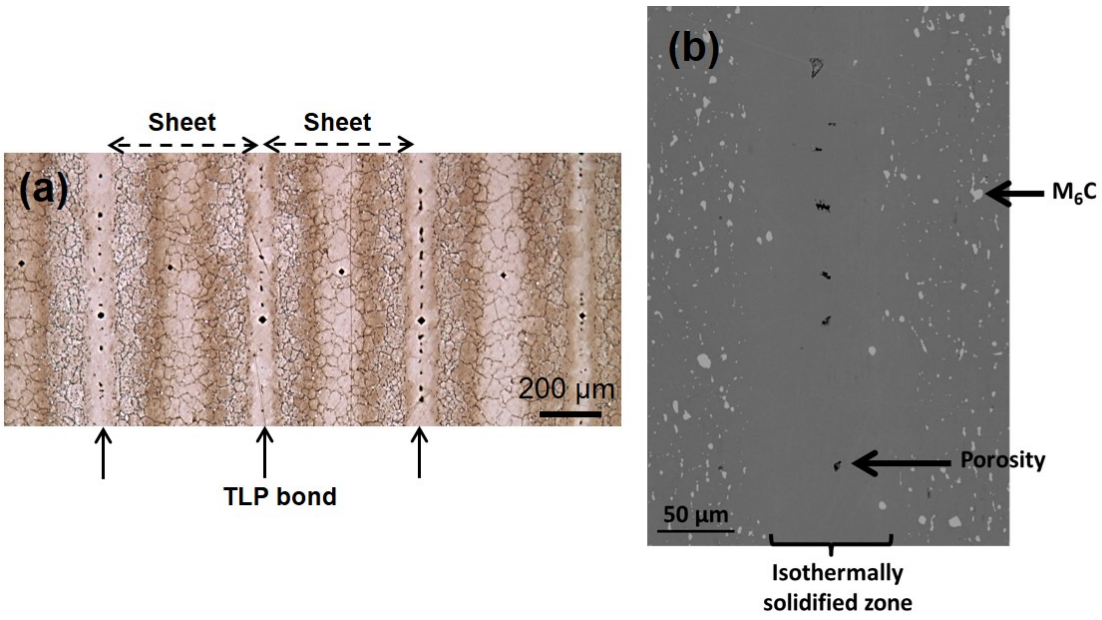

Figure 1. (a) An optical micrograph illustrating several layers of TLP bonded Alloy 230 sheets and (b) an SEM image of a bond region.

X-ray energy dispersive spectroscopy (EDS) composition analysis, to identify a composition gradient across the Alloy 230 sheet and joint region, was performed because Alloy 230 is a solid-solution-strengthened alloy and a composition gradient can alter its strength. Eventually, a composition difference can also result in a different corrosion response to the sCO_2 environment. Fig. 2 shows concentration gradient of phosphorus, which is the MPD, from the bond line to the center of the sheet in Set I and Set II.

Mechanical Properties

Vickers microhardness was used to test the relative strength of the bond (or ISZ) region and the sheet region. Fig. 2 summarizes the hardness (kgf/mm^2) results of the following samples – as-received (AR) Alloy 230 sheet, the middle of the sheet and the joint centerline (bond) in Set I and Set II to be 225 ± 19, 236 ± 12, 183 ± 13, 237 ±13, 191 ± 11 respectively. A couple of details of note – the hardness of the AR sheet is almost similar to the hardness of middle of the sheet (275 µm from the joint centerline) in both Set I and Set II. Second, the hardness of the joint centerline (bond) is approximately 78 % and 80.5 % in set I and set II, respectively compared to that of the middle of the sheet.

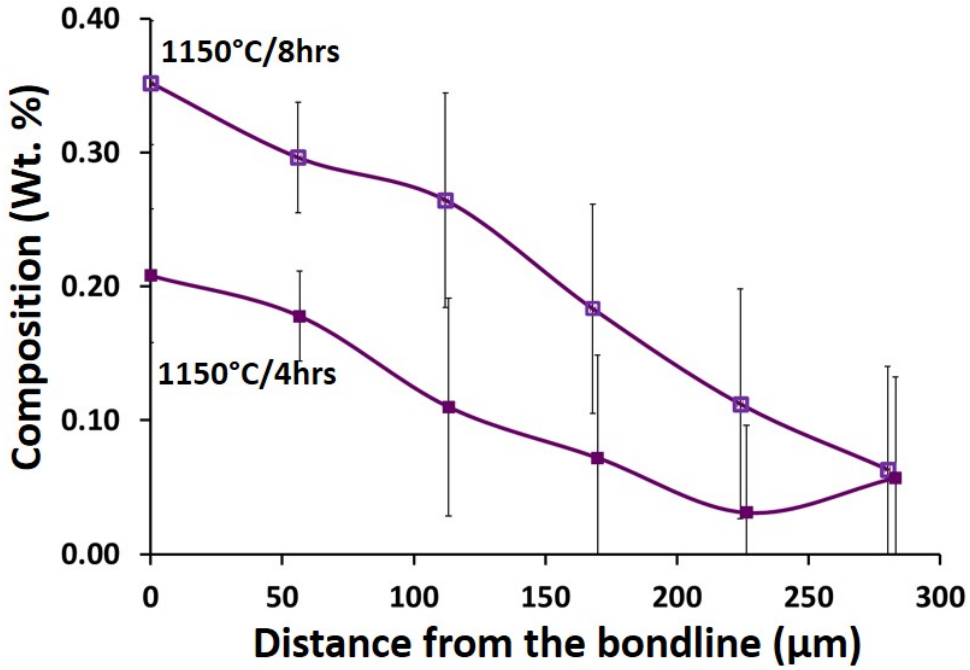

Figure 2. Phosphorus compositional profile from the bond line to the center of the sheet in Set I and Set II. The error bars indicate the standard deviation of the measurements at each location.

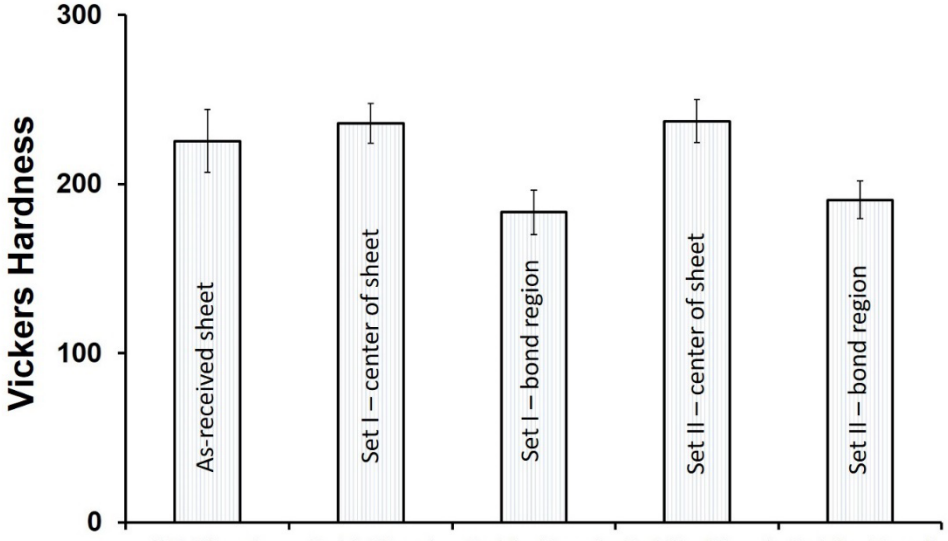

Figure 3. Vickers hardness as measured at various locations in TLP bonded stacks and as-received sheet. The error bars indicate the standard deviation in 10 measurements.

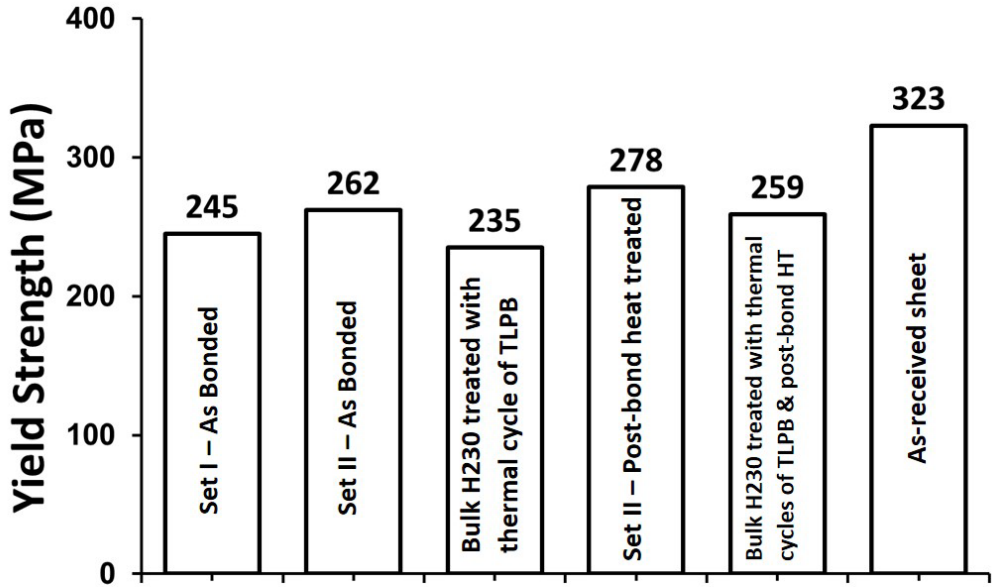

Figure 4. Yield strength of the TLP bonded Alloy 230 stacks and base material as tested at 750°C.

Tensile testing of TLP bonded Alloy 230 stacks was performed at 750°C. Fig. 4 summarizes the yield strength of TLP bonded Alloy 230 stacks, Alloy 230 sheet, and bulk Alloy 230 plate which underwent a thermal cycle that mimics the bonding thermal cycle and the post-bonding heat-treatment thermal cycle. On testing at 750°C, the yield strength of Set I and Set II is ~ 25% and ~ 19% respectively lower than that of the as-received Alloy 230 sheet. The post-bond heat treatment of the as-bonded Set II increased the yield strength to 86% of the as-received sheet. The higher strength after heat treatment can be attributed to the dissolution of the precipitates and therefore putting the strengthening elements into solution to contribute to strengthening. Both sets of the TLPB Alloy 230 achieved strengths similar to the strength of bulk Alloy 230 plate that was heat treated to mimic the TLP bonding and post-bonding heat treatment cycles. Similarly for elongation (not shown here), the TLP bonded

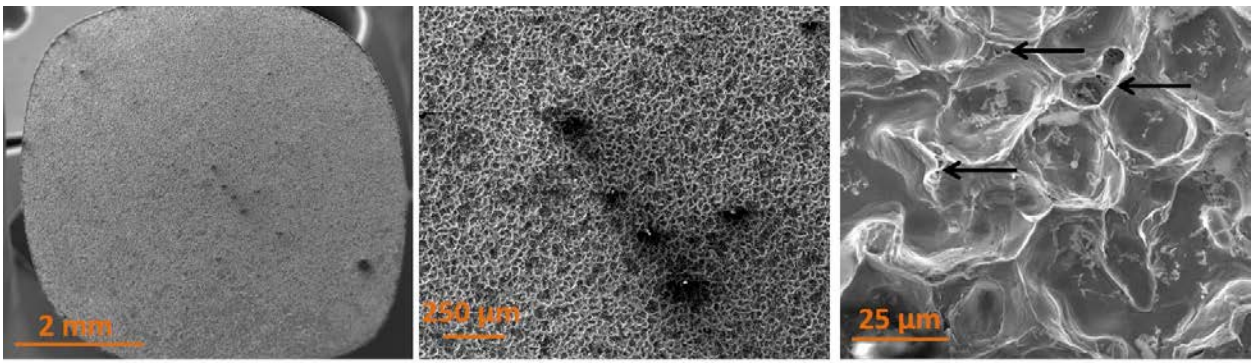

Figure 5. SEM images of fracture surface of a tensile bar from Set II (As-bonded) tested at 750°C Note the porosity in the right most image.

samples show a very limited elongation (approximately 1%) when tested at 750°C. However, the microstructure of the fracture surface of TLP bonded Alloy 230 stacks is consistent with a ductile fracture through the bonded layer, Fig. 5.

Corrosion of bonded materials in CO_2

Average mass change for the monolithic, and TLP-bonded coupons is presented in Fig. 6. The Alloy 230 monolithic coupons (H230-Sheet) showed mass gains which were less than that of the TLP bonded coupons (H230-TLP). The mass for both bonded and monolithic Alloy 230 increases fast during the first 500 h of exposure and slower during the rest of the exposure.

Cross-section examination of the exposed TLP bonded coupons using back-scattered electron (BSE) imaging revealed a thin oxide scale on all of the coupons (Fig. 7). The scale was approximately 1-2 µm thick. A thicker scale was observed above carbide particles near the sample surface. No significant thickness variation was observed between the scale on the bond and the scale on the sheet.

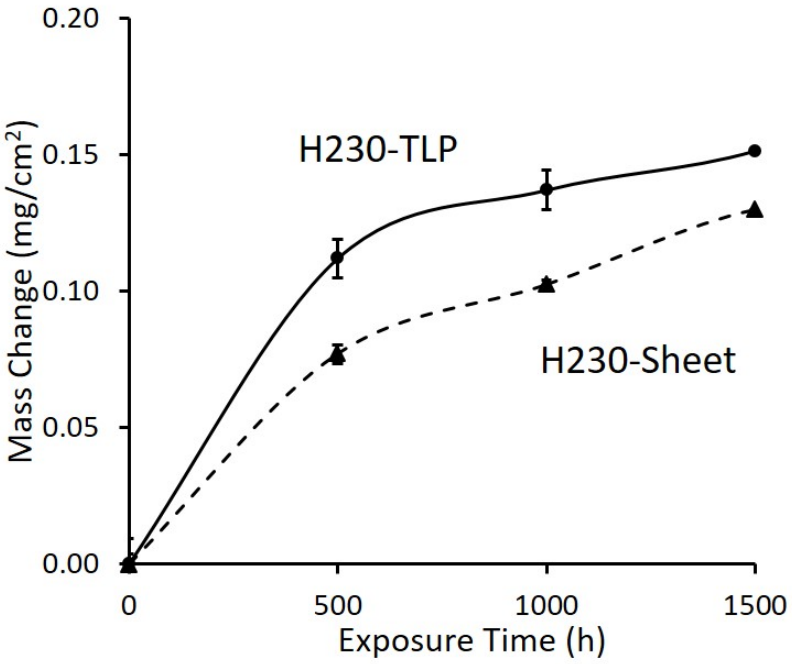

Figure 6. Mass gain due to oxidation of base alloy 230 (H230-Sheet) and TLP bonded Alloy 230 (H230-TLP).

Challenges

To facilitate TLP bonding, the Alloy 230 sheets were plated with Ni-P alloy. P in the Ni-P plating alloy acts as the MPD in the plating and enables the plating to be in a liquid form during bonding at 1150°C. The P diffuses into the sheet while bonding and during the subsequent heat treatment. The high

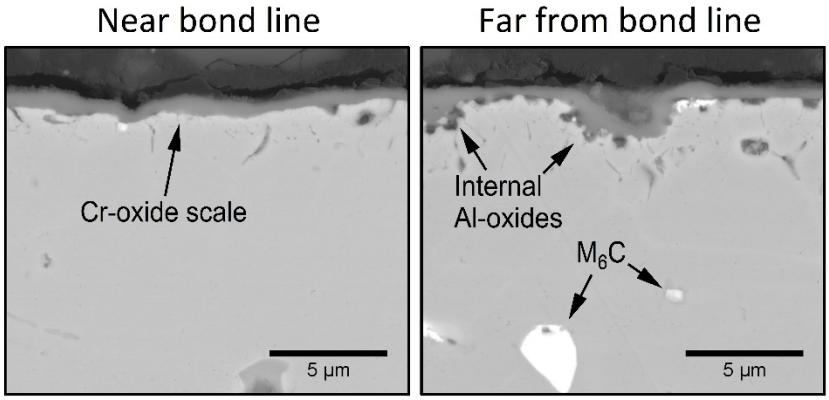

Figure 7. Back-scattered electron (SEM) images of cross-sections of Alloy 230-TLP showing oxide scale growth on the surface near a bond line and far from a bond line (sheet base metal) after 1500 hour exposure to CO_2 at 700°C.

amount of P in Ni-P plating - approximately 12 wt. % P on Set I Alloy 230 sheets - can result in the formation of intermetallic phases in the vicinity of the bondline and a higher amount of P in both the sheet and the bondline. Even though there is no conclusive evidence on the effect of elemental P on the mechanical properties in these alloys, the presence of intermetallics is generally associated with a low toughness. Consequently, the Set II sheets had about 6 wt. % P on each side and no detrimental intermetallic phases have been resolved in the bonded stacks using scanning electron microscopy [Kapoor].

Bonding for long times (for example, 8 h as in Set I) results in a higher (3X) volume fraction of (W,Mo,Ni)-based carbides compared to the as-received Alloy 230 sheets. This is detrimental for the strength of the alloy because a higher amount of solid-solution-strengthening elements (W & Mo) are trapped in the precipitates and therefore cannot provide the strengthening. Therefore, the bonding time should be kept as short as possible to hold the increase in volume fraction of precipitates to a minimum. On the other hand, sufficiently long bonding time is required to have a complete isothermal solidification at the bonding temperature since the solidification depends on the diffusion of phosphorous (or other MPD), a time-dependent process, away from the molten zone into the sheet. In the case of insufficient bonding time, the stack begins to cool down before the isothermal solidification is complete and this may result in formation of intermetallic phases. Consequently, a 4 h bonding time was used in Set II.

TLP bonding of Alloy 230 sheets resulted in isothermally solidified zones (bond regions) that were denuded of second phase of M_6C as shown in Fig. 1b. The lack of M_6C precipitates in the ISZ can be explained with the fact that the chemical composition of ISZ is approaching to that of the matrix of the Alloy 230 sheet due to diffusion of elements in both direction at the bonding temperature. Because the matrix composition is in equilibrium with the composition of M_6C in the sheet at the bonding temperature, the ISZ composition does not support the formation of new M_6C precipitates. Since the M_6C precipitates are very stable up to above 1200°C, a heat treatment to dissolve M_6C, homogenize the composition, and reprecipitate M_6C in both the ISZ and the sheet is not practicable due to concerns of excessive grain growth. The lower strength of the ISZ compared to the sheet (Fig. 3) is due partly to this microstructural difference. The lower strength of the ISZ is likely to result in more localized strain in the

ISZ compared to the sheet material when TLPB stack is loaded perpendicular to the bond plane. This may give rise to shorter creep and fatigue life.

Another concern with the TLPB of Alloy 230 is the presence of pores in the ISZ. These pores were identified as shrinkage pores that formed when the last molten metal solidified [Kapoor]. The shrinkage porosity occurs due to the difference in molar volumes of liquid and solid. It may be hard to find a feasible method to eliminate this porosity in the TLPB process. The porosity is likely to affect mechanical properties of the TLPB stacks negatively. They were observed on the fracture surfaces of the tensile test bars machined from the TLPB stacks as shown by arrows in Figure 5. They can play a detrimental role in fatigue and creep failure of these stacks.

SUMMARY

Stacks of Alloy 230 sheets were joined via TLPB utilizing a Ni-P interlayer. Chemical composition of the bond region (ISZ) was similar to that of the matrix in the sheet. Microstructure of bond region (ISZ) was denuded of M_6C precipitates.

On testing at 750°C, the yield strength of stacks was 19% to 25% lower than that of the as-received Alloy 230 sheet. The post-bond heat treatment of the as-bonded stack increased the yield strength to 86% of the as-received sheet. Although overall elongation was low (about 1%), through the bond layer fracture clearly showed ductile features.

TLP bonded Alloy 230 stacks gained more mass due to oxidation compared to the as-received Alloy 230 sheet in CO_2 at 700°C. However, overall mass gains were low for all samples.

Several challenges characteristic of TLP bonding process of Alloy 230 were identified. They were formation of intermetallic phases, shrinkage porosity, and lack of second phases (M_6C) in the bond region (ISZ).

ACKNOWLEDGEMENTS

This work was performed in support of the U.S. Department of Energy's Fossil Energy (FE) Advanced Turbines and Crosscutting Technology Research Programs and Energy Efficiency and Renewable Energy (EERE) Sunshot Program. This research was supported in part by appointments (MK and RPO) to the National Energy Technology Laboratory Research Participation Program sponsored by the U.S. Department of Energy and administered by the Oak Ridge Institute for Science and Education.

REFERENCES

ASTM standard E8, 2013 “Standard test methods for tension testing of metallic materials” ASTM International, West Conshohocken, PA.

Cook, G.O., Sorenson, C.D., “Overview of Transient Liquid Phase and Partial Transient Liquid Phase Bonding”, Journal of Materials Science, 46 (2011) 5305-5323.

Doğan, Ö.N., Carney, C., Oleksak, R.P., Disenhof, C.R., Holcomb, G.R., “High-Temperature Corrosion of Diffusion Bonded Ni-Based Superalloys in CO_2”, Proceedings of the 5th International Symposium on Supercritical CO2 Power Cycles, March 28-31, 2016, San Antonio, Texas, USA.

Foursprings, P.M., Nehrbauer, J.P., Sullivan, S., Nash, J., “Testing of Compact Recuperators For A Supercritical CO_2 Brayton Power Cycle”, Proceedings of the 4th International Symposium on Supercritical CO2 Power Cycles, September 9-10, 2014, Pittsburgh, Pennsylvania, USA.

Ghazvini, M., Narayanan, V., “A Microscale Combustor Recuperator and Oil Heat Exchanger- Design and Thermofluidic Characterization”, International Journal of Heat and Mass Transfer, 64 (2013) 988-1002.

Haynes 230 Technical Data, http://haynesintl.com/docs/default-source/pdfs/new-alloy-brochures/high-temperature-alloys/brochures/230-brochure.pdf

Hill, A., Wallach, E.R., “Modelling Solid State Diffusion Bonding”, Acta Metallurgica 37 (1989) 9 2425-2437.

Kapoor, M., Doğan, Ö.N., Carney, C.S., Saranam, R.V., McNeff, P.S., Paul, B.K., “Transient-Liquid-Phase Bonding of H230 Ni-Based Alloy using Ni-P Interlayer – Microstructure & Mechanical Properties”, Metallurgical and Materials Transactions A, Accepted, 2017. DOI: 10.1007/s11661-017-4127-5.

Le Pierres, R., Southall, D., Osborne, S., "Impact of Mechanical Design Issues on Printed Circuit Heat Exchangers," Proceedings of the 3rd International Symposium on Supercritical CO2 Power Cycles, May 24-25, 2011, Boulder, Colorado, USA.